BioOne COMPLETE

Is Mini Beam Ready for Human Trials? Results of Randomized Study of Treating De-Novo Brain Tumors in Canines Using Linear Accelerator Generated Mini Beams

Authors: Kundapur, V., Mayer, M., Auer, R. N., Alexander, A., Weibe, S., et al.

Source: Radiation Research, 198(2) : 162-171

Published By: Radiation Research Society

URL: https://doi.org/10.1667/RADE-21-00093.1

BioOne Complete (complete.BioOne.org) is a full-text database of 200 subscribed and open-access titles in the biological, ecological, and environmental sciences published by nonprofit societies, associations, museums, institutions, and presses.

Your use of this PDF, the BioOne Complete website, and all posted and associated content indicates your acceptance of BioOne's Terms of Use, available at www.bioone.org/terms-of-use.

Usage of BioOne Complete content is strictly limited to personal, educational, and non - commercial use. Commercial inquiries or rights and permissions requests should be directed to the individual publisher as copyright holder.

BioOne sees sustainable scholarly publishing as an inherently collaborative enterprise connecting authors, nonprofit publishers, academic institutions, research libraries, and research funders in the common goal of maximizing access to critical research.

Downloaded From: https://bioone.org/journals/Radiation-Research on 11 Aug 2024
Terms of Use: https://bioone.org/terms-of-use

RADIATION RESEARCH **198**, 162–171 (2022)
0033-7587/22 $15.00
©2022 by Radiation Research Society.
All rights of reproduction in any form reserved.
DOI: 10.1667/RADE-21-00093.1

Is Mini Beam Ready for Human Trials? Results of Randomized Study of Treating De-Novo Brain Tumors in Canines Using Linear Accelerator Generated Mini Beams

V. Kundapur,[a] M. Mayer,[b] R. N. Auer,[c] A. Alexander,[d] S. Weibe,[e] M. J. Pushie,[f] G. Cranmer-Sargison[d]

[a] Radiation Oncology, Saskatchewan Cancer Agency, Saskatoon Cancer Centre, Saskatoon, SK Canada S7N4H4; [b] Veterinary Radiation Oncology, Department of Small Animal clinical Sciences and [c] Department of Pathology and Laboratory Medicine, University of Saskatchewan, Saskatoon, SK Canada S7N 0W8; [d] Radiation Physics, Saskatchewan Cancer Agency, Saskatoon Cancer Centre, Saskatoon, SK Canada S7N4H4; and [e] Department of Clinical Imaging and [f] Department of Surgery, University of Saskatchewan, Saskatoon, SK Canada S7N 0W8

Kundapur V, Mayer M, Auer RN, Alexander A, Weibe S, Pushie MJ, Cranmer-Sargison G. Is Mini Beam Ready for Human Trials? Results of Randomized Study of Treating De-Novo Brain Tumors in Canines Using Linear Accelerator Generated Mini Beams. Radiat Res. 198, 162–171 (2022).

The main challenge in treating malignant brain neoplasms lies in eradicating the tumor while minimizing treatment-related damage. Conventional radiation treatments are associated with considerable side effects. Synchrotron generated micro-beam radiation (SMBRT) has shown to preserve brain architecture while killing tumor cells, however physical characteristics and limited facility access restrict its use. We have created a new clinical device which produces mini beams on a linear accelerator, to provide a new type of treatment called mini-beam radiation therapy (MBRT). The objective of this study is to compare the treatment outcomes of linear accelerator based MBRT versus standard radiation treatment (SRT), to evaluate the tumor response and the treatment-related changes in the normal brain with respect to each treatment type. Pet dogs with de-novo brain tumors were accrued for treatment. Dogs were randomized between standard fractionated stereotactic (9 Gy in 3 fractions) radiation treatment vs. a single fraction of MBRT (26 Gy mean dose). Dogs were monitored after treatment for clinical assessment and imaging. When the dogs were euthanized, a veterinary pathologist assessed the radiation changes and tumor response. We accrued 16 dogs, 8 dogs in each treatment arm. In the MBRT arm, 71% dogs achieved complete pathological remission. The radiation-related changes were all confined to the target region. Structural damage was not observed in the beam path outside of the target region. In contrast, none of the dogs in control group achieved remission and the treatment related damage was more extensive. Therapeutic superiority was observed with MBRT, including both tumor control and the normal structural preservation. The MBRT findings are suggestive of an immune related mechanism which is absent in standard treatment. These findings together with the widespread availability of clinical linear accelerators make MBRT a promising research topic to explore further treatment and clinical trial opportunities. © 2022 by Radiation Research Society

[1] Address for correspondence: Dr. Vijayananda Kundapur, Clinical Professor, College of Medicine, University of Saskatchewan, Saskatoon Cancer Centre, Saskatoon, S7N4H4, SK, Canada; e-mail: Vijayananda.kundapur@saskcancer.ca.

INTRODUCTION

The challenge in treating malignant brain neoplasms lies in eradicating the tumor while minimizing treatment-related damage to normal adjacent brain. Conventional radiation therapy of brain tumors relies on the radiobiological principle of temporal fractionation to exploit the differences in the ability of malignant cells and normal tissue cells to repair radiation damage. Conventional radiation therapy is administered in a series of 1.8–2.66 Gy daily doses or fractions, for a period of approximately 4 to 6 weeks (1–3). While this has dramatically increased physicians' ability to cure or provide long-term tumor control of many cancers, there are some tumors such as high-grade gliomas of the brain, for which the prognosis remains grim (3). Conventional radiation therapy is also associated with collateral damage to normal brain tissue (4). In long-term survivors, this may manifest as varying combinations of neurocognitive/neuropsychological problems and/or impaired bone growth. These clinical manifestations can be correlated to the imaging changes on follow up scans (5), and further explained on pathological examination of the brain adjacent or away from the targeted lesion. On necropsy studies, the treated regions show dose dependent changes ranging from minimal to complete avascular necrosis, extensive vacuolization in brain parenchyma along with rarefaction of the blood vessels (6–9). An elegant study elucidating long-term radiation effects on normal brain tissue as a function of dose and time showed the possibility of neuroinflammation as the basis for the long-term side effects of radiation (10). Most of the late radiation damage may be the consequence of ongoing radiation related changes in the vascular endothe-

Downloaded From: https://bioone.org/journals/Radiation-Research on 11 Aug 2024
Terms of Use: https://bioone.org/terms-of-use

lial fabric network of the brain (11). However, irrespective of the underlying mechanism of action, mitigating the toxicity related to radiation treatment while eradicating the tumor is currently an unmet goal in the treatment of brain tumors. The dose of radiation to the brain during conventional radiation therapy for controlling or killing brain tumor cells has always been limited by the normal tissue tolerance and treatment-related long-term morbidities, underscoring the need for better or newer modalities of treatment (4).

Spatial fractionation radiation treatment using arrays of narrow, parallel micro-beams, has been explored extensively using synchrotron-generated X rays. With synchrotron-generated micro-beam radiation therapy (SMBRT), there are two main regions of dose distribution; the path of the micro-beam, or peak, and the tissue that is not directly traversed by the micro-beam, or valley. Beam width ranging from tens of microns up to 950 μm has been reported (12). Slatkin et al. demonstrated preservation of cellular integrity after SMBRT even at very large doses (13). Dilmanian et al. and Serduc et al. further showed the normal tissue-sparing effects of micro-beam radiation treatment on the brain (14, 15). When spatial fractionation is used, normal brain tissue has been shown to tolerate peak entrance doses of several hundred Gy with preservation of cognitive function clinically, and post-mortem neural architecture structurally (13–18).

It has been theorized that normal brain tissue tolerance to SMBRT is related to the spatial fractionation of the radiation, which allows rapid repair of damage by neighboring endothelial and glial cells (19, 20). Micro-beams not only have potential for greater sparing of normal tissue, but are also more damaging to malignant tissues, with a superior therapeutic ratio (13, 14, 21, 22). However, the radiobiological mechanisms are not understood conclusively, with several competing theories concerning both immune response and chemical reaction pathways (13, 14, 21–23). Nevertheless, it is clear from SMBRT studies that spatially fractionated micro-beams offer an advantage over conventional radiation therapy.

To extrapolate the knowledge learned from SMBRT studies and move towards human use, in 2009 a tungsten collimator was designed to produce a beam of 1,000 μm size that was named a ''mini beam'', and could be used with an RT-250 superficial X-ray machine (24). This was the first step towards realizing the goal of using this new medical technology for the treatment of human cancers. Based on the findings from our bridging study done between the years, 2011 and 2013, with a view to transfer the therapeutic advantage of SMBRT to larger animals and possibly to human brain tumor treatment, a linear accelerator mounted mini-beam collimator for use at a nominal 6 MV beam energy was designed and characterized (25–27).

The mini beams generated on a linear accelerator (megavoltage mini beams) have potential advantages over kilovoltage beams generated on a synchrotron, with a comparatively higher energy that allows radiation to reach deeper targets within the patient while reducing the surface dose. Synchrotron beams generally cannot deliver radiation to targets at 6–10 cm depths without a significant surface dose. Nevertheless, synchrotron beams can have greater control of beam shape with a higher radiation intensity, but can be more limited in terms of availability for regular use compared to megavoltage radiation sources. Megavoltage mini beams also differ significantly from either kilovoltage beams or ''classical'' micro beams produced at synchrotron facilities in terms of beam geometry, peak-to-valley dose ratio (PVDR) and depth-dose characteristics. The megavoltage mini-beam collimator used in this work is the same physical device that has been described by Davis et al, and consists of 30 tungsten blades with 0.6 mm width and 10 cm length held in an aluminum frame and arranged to produce planar mini beams 1 mm thick with a maximum field size of 5×5 cm (27). The collimator assembly is mounted directly to the linac gantry head using a standard accessory mount. From ref. 29, using this collimator results in dose peaks with full width at half maximum (FWHM) of 1.0 mm at isocenter. The FWHM is relevant because megavoltage mini beams take a profile with a sharp peak widening towards the base, as opposed to synchrotron beams which are quasi-parallel. The PVDR of megavoltage beams is found to decrease with depth, but is still significant at a 10 cm depth while maintaining a low-surface dose. Both the FWHM and PVDR of megavoltage beams have a further dependence on the spot size of the initial electron beam, and are therefore dependent on the specific linac used. Due to these factors, the PVDR of the megavoltage mini-beam collimator in this work was found to be $\sim$1.47 at a 10 cm depth in water when averaging across results from 3 different machines (25, 27). This is significantly lower than the PVDR typically seen for synchrotron beams, which can be as high as 48 when 25 μm wide beams are used (19). It has been proposed that a higher PVDR results in lower normal tissue toxicity (15), but there is no known direct relationship between PVDR number and ultimate treatment efficacy.

With the megavoltage collimator available, this study aimed to examine animals larger than mice that are typically used in micro beam studies. Smaller laboratory animal studies have many pitfalls that were revealed in our initial study, including the disproportionate size of rapidly growing transplanted tumors compared to the actual small size of the brain, resulting in a short life span for these animals. This short follow-up time postirradiation precludes the gathering of information on tumor response or long-term side effects of radiation.

To obtain more illuminating results using larger animals, this study compared megavoltage mini-beam radiation treatment (MBRT) to standard radiation treatment (SRT) of naturally occurring brain tumors in pet dogs. Primary nervous system tumors arise spontaneously in companion

Downloaded From: https://bioone.org/journals/Radiation-Research on 11 Aug 2024
Terms of Use: https://bioone.org/terms-of-use

animals as in human patients, and radiation therapy is the standard treatment for most of these tumors. Client-owned dogs provide an excellent model for studying the response of normal brain and tumor to MBRT. Similar to humans, dogs have gyrencephalic brain whereas small animals like mice have lissencephalic brain. Dogs can present with naturally occurring tumors which mimic the biological behavior and complex tumor microenvironment of spontaneous human tumors. (28) Additionally, the response of canine brain tissue to radiation is similar to that of human brain tissue, and the physical dimensions of the dog brain and skull are closer to those of human patients than small rodents. Side effects in irradiated normal tissues can occur years after irradiation and limit the total dose that can be administered to a tumor. Pet dogs can be followed for long periods of time, up to their remaining lifespan, while having neurological and imaging examinations to assess for signs of tumor recurrence and long-term-side effects. Owners are generally able to give detailed information on the daily quality of life achieved after irradiation, as well as on subtle cognitive changes that may not be apparent upon a single examination by a veterinarian.

Objective

The objective of this study is to compare the treatment outcomes of linear accelerator based MBRT vs. SRT, to evaluate the tumor response and the treatment-related changes in normal brain tissue with respect to each treatment type.

MATERIALS AND METHODS

Treatment Arms

This study was approved by the local Animal Ethics Research Board of University of Saskatchewan, Canada, in accordance with best practices set by the Canadian Council on Animal Care. Pet dogs with spontaneously developed brain tumors were recruited for the study. These dogs were evaluated clinically using magnetic resonance imaging (MRI). Presumptive diagnosis was done based on the imaging study, with the results detailed in Table 2. None of the dogs underwent biopsy as per standard of practice. Upon completion of staging workup, the dogs were randomized to receive SRT vs. MBRT. All the dogs were anesthetized and immobilized using a vacuum-deformable body cushion. A thermoplastic neck cushion ventral to the head and cervical region was used along with a custom-made indexed maxillary plate, thermoplastic bite block and a thermoplastic head mask dorsal to the head region. Control dogs received standard radiation treatment of 9 Gy on 3 consecutive days for a total dose of 27 Gy (Fig. 1e–g and Table 1, SRT). The treatment was distributed using 5 entry ports delivered by rotating the linac gantry to fixed angles determined by the treatment planning system. Dogs in the investigational MBRT arm received a single 26 Gy fraction mean dose to the target (Fig. 2 g–i; Table 1, MBRT). In the case of MBRT the use of ''mean dose'' was adapted to refer to the whole target and is defined by the difference between the dose where the beamlet is traversing compared to where it is not. Due to this fact point doses are shown in Fig. 2g–i that are higher than 26 Gy due to the peak and valley dose distribution of the mini beams. The treatment type used can be defined as multiple port intersecting mini beams, and was delivered using 2 entry ports as shown in Fig. 2g. All dogs were maintained on steroid and anti-epileptic medications as needed. After the treatment, the dogs were followed at regular intervals by the referring veterinarian for clinical assessment. Dogs also had a follow-up MRI every 3 months. The images were evaluated by one neuroradiologist (SW). Depending on the decision of the owner of these pet animals, they were euthanized, and brains were obtained for centralized evaluation by a single veterinary neuropathologist (BP).

X-Ray Fluorescence Imaging

Synchrotron-based X-ray fluorescence imaging (XFI) was performed at the Stanford Synchrotron Radiation Light source on beamline 10-2, with the SPEAR3 storage ring operating in top-up mode at 3 GeV and 500 mA, following established methods (29). Beamline 10-2 was equipped with a 33-pole 1.45-Tesla wiggler, using a Si(111) double-crystal monochromator ($\phi = 90°$ orientation) and a Rh-coated mirror for focusing. A micro-focussed beam, approximately 35×35 μm, was achieved using an aperture downstream of the I_0 ion chamber. Samples were mounted at 45° to the incident beam and raster scanned using Newport IMS Series stages (Irvine, CA) in 30 μm steps, providing an oversampling pixel size of 30 μm, using a dwell time of 200 ms per point. An incident energy of 13,450 eV was employed, and X-ray fluorescence was detected with a silicon-drift Vortex detector positioned 45° to the sample normal (90° to the incident beam). Multi-channel array spectra for each pixel in the XFI map were processed using the Micro Analysis Toolkit SMAK (30).

RESULTS

A total of 16 dogs were treated in the study, 8 animals per group between the years 2013 and 2017. The initial diagnosis and lesion characteristics for each dog based on the MRI are shown in Table 1, as determined prior to radiation treatment. The lesions were denoted as ''well defined'' if the lesion borders could be clearly visualized. They are labelled ''ill defined,'' if the borders could not be clearly visualized on the MRI. By location of the tumors both groups were having equal proportion (50%) of tumors located on either side of the tentorium. Among the standard radiation treatment group only 2 out of 8 dogs showed features suggesting an aggressive nature tumor (dogs 2 and 5) with brain parenchymal invasion compared to 7 out of 8 dogs in MBRT group (dogs 10 to 16) showing aggressive features including brain parenchymal invasion or invasion into the canal in the base of skull.

Two dogs treated in the standard radiation treatment arm had to be euthanized a short time after the treatment, 1 within 48 h and 1 at day 45. Similarly, 1 dog in the MBRT arm had to be euthanized within 48 h (Table 2). The autopsy study of these 3 dogs showed aspiration pneumonia and sepsis as the cause for death. Following assessment, these were all deemed unrelated to the treatment, and therefore these 3 dogs were not included in the final analysis. The remaining dogs in the study in both arms were euthanized during follow-up at the discretion of their owners depending on their symptoms and how they were thriving.

Clinical Evaluation During Follow-up

The overall survival ranged from 45 to 1,500 days for the standard radiation treatment group, 150 days to 1,080 days

Downloaded From: https://bioone.org/journals/Radiation-Research on 11 Aug 2024
Terms of Use: https://bioone.org/terms-of-use

TABLE 1
Lesion Location and Characteristics Prior to Radiation Treatment Determined from MRI

Patient	Treatment type	Location	Lesion characteristics	Pre-radiation treatment size (cm)	Tumor volume in CC
1	SRT	Mid cranial fossa, dural based	Well defined	1.4 × 0.9 × 1.5	1.08
2	SRT	Left temporal lobe, invading parenchyma	Heterogenous, necrosis, edema	1.2 × 1.1 × 2.4	1.05
3	SRT	Dorsal caudal aspect of 3rd ventricle	Well defined, no necrosis, no edema	0.4 × 0.6 × 0.4	0.17
4	SRT	Posterior fossa, behind brain stem, dural based,	Ill defined, no necrosis, edema	1.2 × 3.1 × 2.6	5.38
5	SRT	Midbrain near Thalamus, invading brain parenchyma	Well defined, no necrosis, no edema	1.3 × 1.5 × 1.4	1.68
6	SRT	Frontal lobe, olfactory bulb, dural based	Well defined, edema, no necrosis	2.0 × 1.6 × 1.0	4.12
7	SRT	Skull base near foramen magnum, post fossa, dural based	Well defined, no necrosis, no edema	0.5 × 1.4 × 2.5	2.17
8	SRT	Posterior to brainstem in posterior fossa, dural based	Ill defined, no edema, no necrosis	1.6 × 1.5 × 1.0	1.78
9	MBRT	Right frontal lobe, dural based	Well defined, edema, no necrosis	1.3 × 1.0 × 1.9	2.35
10	MBRT	Left posterior fossa, extending to internal auditory canal, dural based	Well defined, minimal edema, no necrosis	2.8 × 1.0 × 1.0	4.38
11	MBRT	Brain stem and cerebellar peduncle, invading brain parenchyma	Ill defined, possible necrosis, edema	1.6 × 1.3 × 2.3	1.59
12	MBRT	Right Cerebellar, invading brain parenchyma	Well defined, minimal edema, no necrosis	1.4 × 1.5 × 1.0	4.27
13	MBRT	Left frontal lobe, invading brain parenchyma, olfactory bulb	Well defined, edema, no necrosis	1.4 × 2.6 × 1.8	5.67
14	MBRT	Frontal lobe, invading brain parenchyma	Ill-defined ring enhancing, edema, no necrosis	1.3 × 1.2 × 1.2	3.25
15	MBRT	Left cerebellar	Well defined, minimal edema, multi cystic, no necrosis	1.6 × 1.7 × 1.0	1.67
16	MBRT	Frontal lobe invading brain parenchyma	Ill-defined ring enhancing, edema, no necrosis	1.3 × 1.2 × 1.2	2.52

Abbreviations: SRT = Standard radiation treatment; MBRT = Megavoltage mini-bean radiation treatment.

for the MBRT group. The median and mean survival was 710 days and 652 days, respectively, for standard radiation treatment group. The median and mean survival for MBRT group was 210 days and 384 days, respectively. Full results for all dogs individually are reported in Table 2. During the first 2 months of follow-up there was no significant difference observed between the two treatment arms, in terms of their symptoms or the medications required. However, clinical evaluation beyond 2 months showed seizure was the more predominant symptom among the

TABLE 2
Tumor Types and Response to Treatment

Patient	Treatment type	Clinical diagnosis from imaging	Number of days after treatment	Final pathology	Response
1	SRT	Ependymoma	78	Choroid plexus carcinoma	PR
2	SRT	Ependymoma	2	Ependymoma	PR*
3	SRT	Ependymoma	1,020	Ependymoma	PR
4	SRT	Meningioma	360	Meningioma	PR
5	SRT	Meningioma	45	Choroid plexus carcinoma	PR^{+}
6	SRT	Meningioma	1,500	Meningioma	PR
7	SRT	Meningioma	900	Meningioma	PR
8	SRT	Meningioma	819	Meningioma	PR
9	MBRT	Meningioma	210	Choroid plexus carcinoma	PR
10	MBRT	Meningioma	150	Meningioma	PR
11	MBRT	Meningioma	2	Meningioma	PR*
12	MBRT	Meningioma	180	No tumor seen	**pCR**
13	MBRT	Meningioma	570	No tumor seen	**pCR**
14	MBRT	Meningioma	240	No tumor seen	**pCR**
15	MBRT	Meningioma	1,080	No tumor seen	**pCR**
16	MBRT	High-grade glioma	240	No tumor seen	**pCR**

Abbreviations: PR = Partial remission (examination under microscope at any magnification revealed the presence of residual brain tumor); pCR = Pathological complete remission (no residual tumor visible under the microscope at any magnification).

* Animal was euthanized within 48 h postirradiation (death not attributed to treatment).

$^{+}$Animal died within 45 days postirradiation (death not attributed to treatment).

Downloaded From: https://bioone.org/journals/Radiation-Research on 11 Aug 2024
Terms of Use: https://bioone.org/terms-of-use

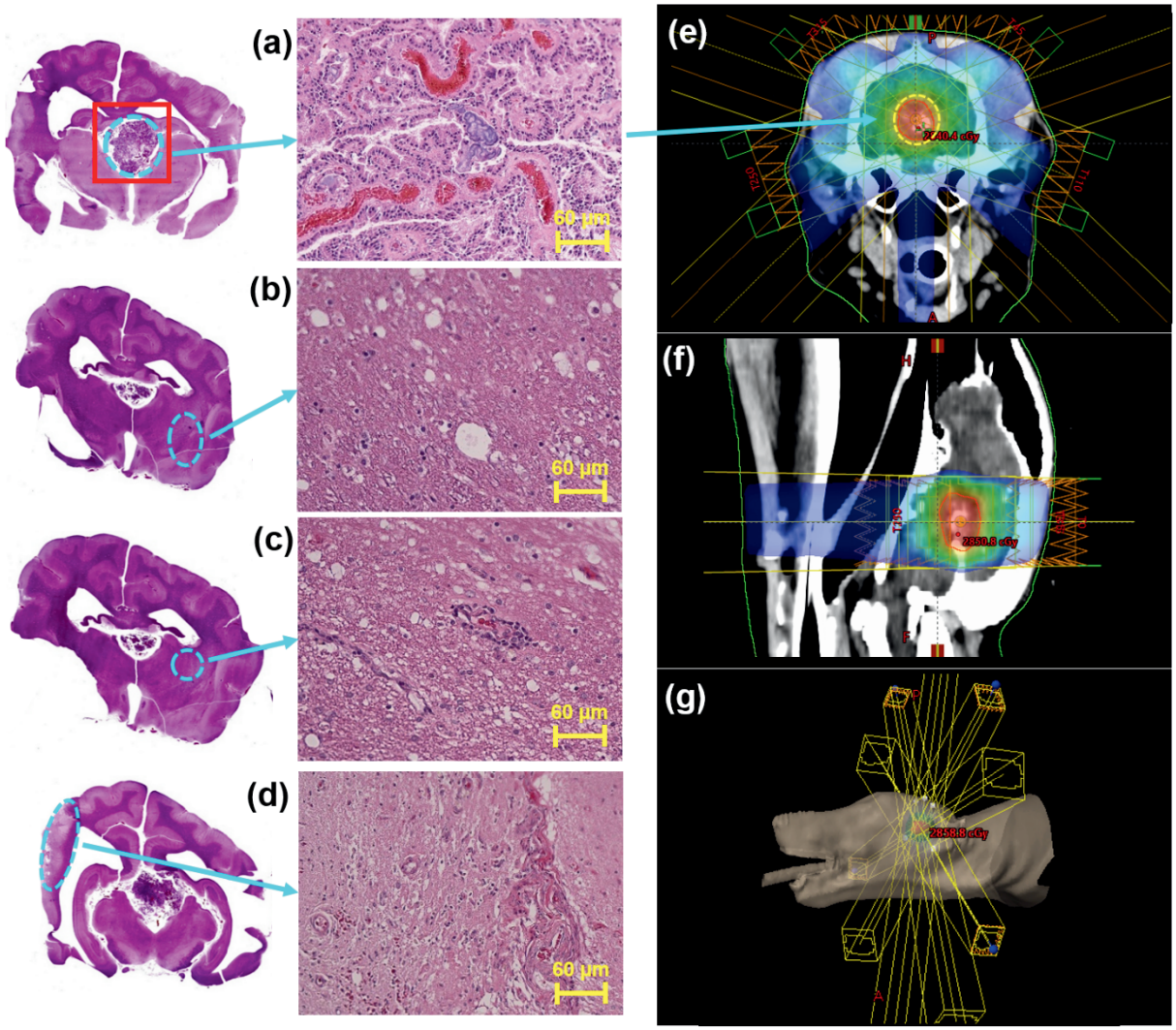

FIG. 1. Brain sections of a dog treated with standard radiation treatment. Staining was accomplished using hematoxylin. The red box indicates the targeted region. Regions outlined in blue circles are shown in magnified images. The right panels show the treatment plan with beam path and dose cloud, as well as the treatment position of the dog. Panel a: Imaging of the targeted region shows persisting residual tumor with viable tumor cells. Panel b: Shows a region remote from the region targeted with standard radiation treatment, showing large amounts of radiation changes with vacuolations and extensive edema. Panel c: Image of the region just outside the targeted area show radiation related changes and rarefaction of vessels with micro-vessels showing perivascular infiltrates. Panel d: Shows more advanced radiation necrotic changes and radiation-induced encephalomalacia is seen in areas quite far removed from treated area, receiving less than 50% of radiation dose. Panel e: Shows an axial slice of the patient with the five entry ports (yellow rectangles) used for treatment as well as the dose color map with a point dose of 2,540.4 cGy within the target region. The entry ports are defined by the rotation angle of the linac gantry, labeled in red text. The mean dose to the peak-to-valley in this case was 2,702 cGy. Panel f: Shows the same patient as panel e from a sagittal perspective with included dose map and a point dose of 2,850.8 cGy shown. Panel g: Shows the 3D model of the same patient and five entry ports outlined in yellow along with a point dose of 2,858.8 cGy shown. The pattern used to collimate the radiation field is marked by a yellow outline at the end of each of entry ports.

MBRT dogs compared to the standard radiation treatment group, while progressively worsening of existing neurological deficits or new neurological symptoms were more predominant in control arm (standard radiation treatment) dogs compared to MBRT group.

Follow-up Imaging analysis

Follow-up images showed tumor response at varying time intervals in the MBRT group, including complete response in 2 dogs. There was treatment-related edema noted in 2/7 dogs. One dog that received MBRT showed changes suggestive of tumor necrosis versus recurrence on follow-up imaging. This has been confirmed upon necropsy study as radiation necrosis was present with no visible tumor. Among the standard radiation treatment group, 2 dogs did not have follow-up imaging as the owners declined follow up imaging. By comparison, tumors persisted in all standard radiation treatment dogs (4/4) with minimal shrinkage noted in only 2 dogs. Treatment-related brain edema changes in the standard radiation treatment arm were noted in 2 of the 4 dogs.

Downloaded From: https://bioone.org/journals/Radiation-Research on 11 Aug 2024
Terms of Use: https://bioone.org/terms-of-use

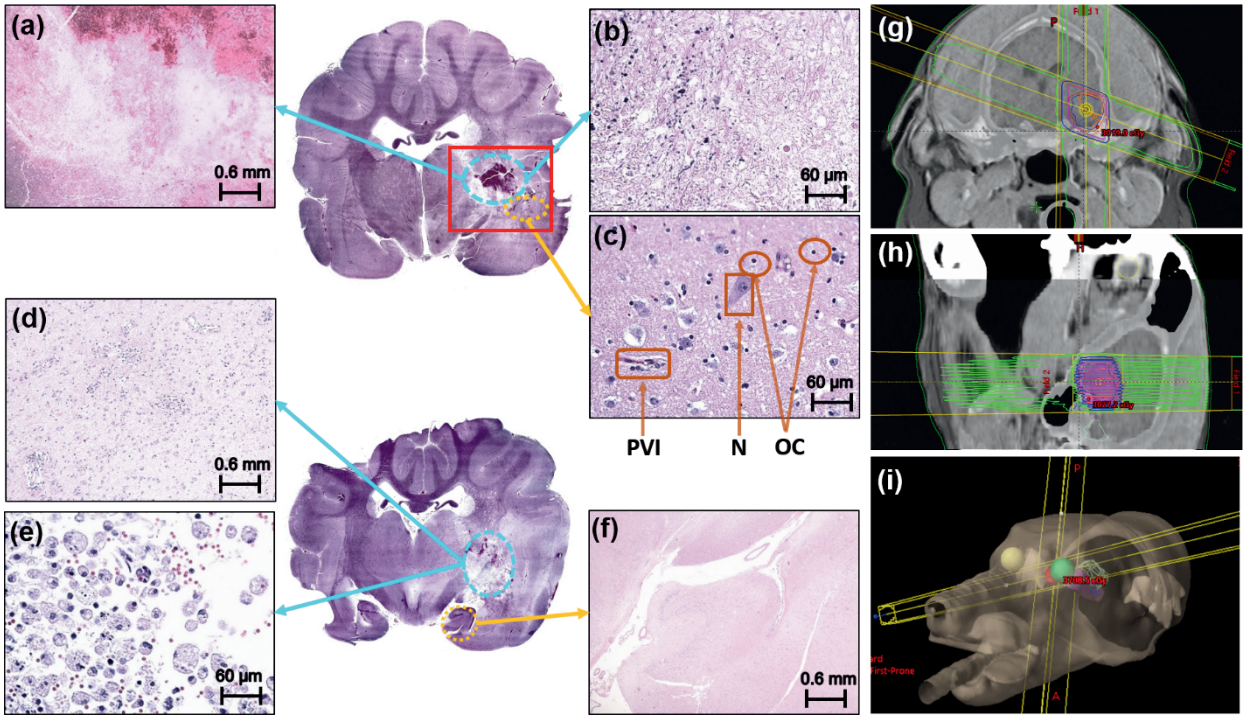

FIG. 2. Sections of dog brain treated with mini beam (MBRT) along with the treatment plan showing the beam path and isodose lines and the treatment position of the dog. Staining was accomplished using hematoxylin. The red box indicates the area targeted for treatment with MBRT. Panel a: Images of the targeted region show pan-necrosis in the area where tumor was situated, and at greater magnification in panel b, the same area shows karyorrhectic debris with no surviving tumor cells. Even inside the region targeted by MBRT, the area imaged in panel c shows surviving neural cells (N), and oligodendrocytes (OC) adjacent to treatment related vacuolation. Also seen is perivascular infiltration in a micro-vessel (PVI). Panel d: Shows the target region with clear evidence of perivascular lymphocyte infiltrates and infiltrates in parenchyma as well as gliofibrillary regeneration. Further magnification in panel e shows macrophage infiltration in the treated region. The region shown in panel f represents the hippocampus which is ~6 mm from the targeted region, and shows intact nuclear layers with no radiation changes. Panel g: Shows an axial slice of the patient with the two entry ports (yellow rectangles) used for treatment as well as the dose color contours with a point dose of 3,019.0 cGy shown within the target region. The mean dose to the peak-to-valley shown was 2,771 cGy in this case. Panel h: Shows the same patient from a sagittal perspective with included dose lines clearly showing the peak-valley pattern of the mini beams, with a point dose of 3,027.2 cGy shown. Panel i: Shows the 3D model of the patient and the two entry ports used and a labeled point dose of 3,708.5 cGy.

Synchrotron X-ray fluorescence imaging on the MBRT dog brain showed preservation of normal structural anatomy at in the brain immediately adjacent to the target area as well as along the path of the beam.

Pathological Evaluation

Neuropathological analysis revealed that all the dogs in the control group treated with standard radiation treatment displayed residual brain tumor during examination under microscope at any magnification (Table 2), a situation which was labeled as ‘‘partial response’’ (PR). A situation in which no residual tumor was visualized under any magnification was denoted as ‘‘pathological complete response’’ (pCR). None of the dogs treated with standard radiation treatment showed pCR, i.e., 0% pCR. There were extensive mitotic figures seen, and macrophage infiltration was noted in the residual tumor as seen in Fig. 1a. Widespread vacuolar edema, in the form of vacuolations, was seen in both white matter and gray matter (Fig. 1b and c). Radiation treatment-related changes outside the targeted area can also be seen. Encephalomalacia was noted even in regions of the brain that received lower doses than 50% (Fig. 1d). There was rarefication of vessel density along with few perivascular or parenchymal inflammatory cell infiltrations (Fig. 1c).

By comparison, the MBRT dogs showed excellent response, excluding the dog that was euthanized within 48 h of treatment, with 71% (5/7) of dogs showing no residual tumor, indicating pCR. Even the dog that was euthanized early within 48 h of treatment, had also shown tumor necrosis and reduction in tumor size. The remaining 2 dogs (2/7) that achieved partial remission, showed few residual tumor cells. One dog showed hemorrhagic necrosis in the tumor bed (Fig. 2a) similar to what has been reported by Tiller-Borcich et al. (31).

Among the dogs designated with pCR, the tumor bed region showed only karyorrhectic debris (Fig. 2b), with lymphocyte and macrophage infiltration (Fig. 2d and e). The microvasculature in this region also showed fibrinoid necrosis in the vascular walls along with lymphocyte infiltration. The density of lymphocyte infiltration was more florid in perivascular regions (Fig. 2c and d). Lymphocyte infiltration was also seen in the meninges and in the brain parenchyma.

Downloaded From: https://bioone.org/journals/Radiation-Research on 11 Aug 2024
Terms of Use: https://bioone.org/terms-of-use

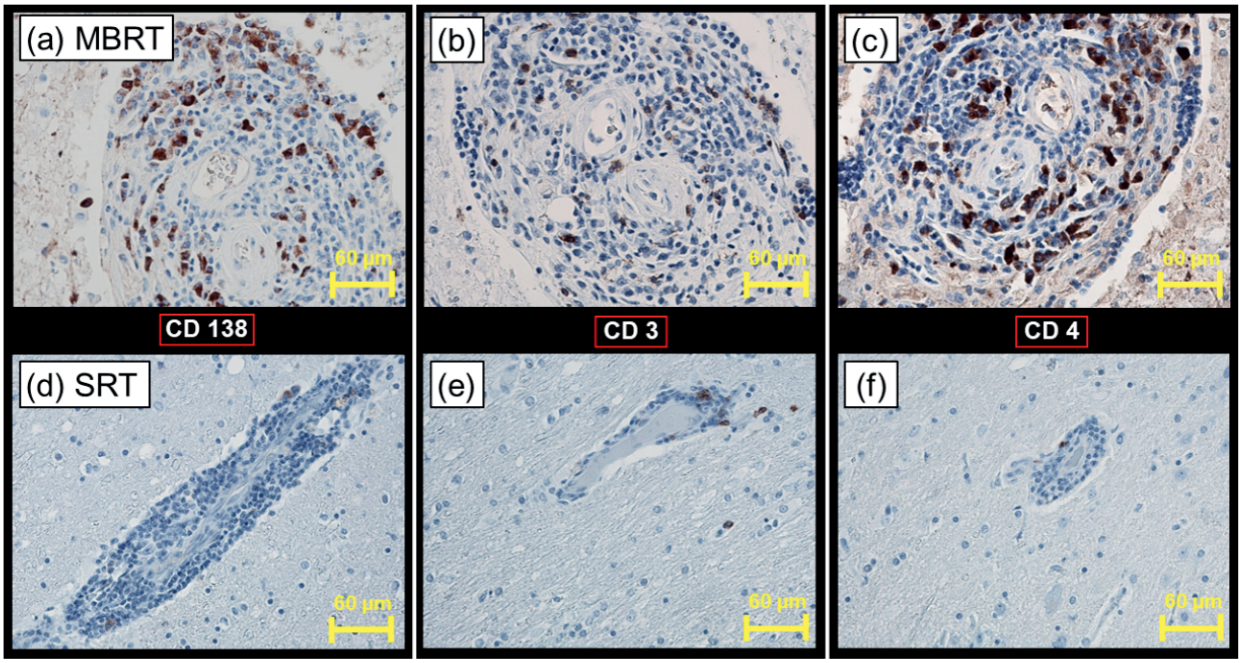

FIG. 3. Comparative immuno-staining for mini-beam radiation treatment (MBRT) on the top row vs. standard radiation treatment (SRT) on the bottom row. Panel a with immunohistochemistry (IHC) staining for plasma cells using the CD138 antibody clearly shows positive staining for infiltrating plasma cells. The corresponding standard radiation treatment image, panel d, shows almost no staining for plasma cells. Similarly in panels b and e, T lymphocytes using CD3 antibody clearly shows positive staining for infiltrating T lymphocytes in dogs treated with MBRT, while almost none is seen when standard radiation treatment is used. Last, panels c and f with IHC staining for CD4 lymphocytes once again shows infiltrating CD 4 lymphocytes in dogs treated with MBRT with almost no staining in control dogs.

Among the MBRT dogs, white matter vacuolation was noted in close proximity to the target area (Fig. 2b and c). However, there were features of gliofibrillary activation/repair in the area. Similarly, there were intact neural cells in the targeted area, months after the treatment, suggestive of neuropil recovery (Fig. 2c). All the radiation-induced changes were confined to the area that received >50% dose, closer to the area that was targeted with MBRT. The rest of the brain traversed by MBRT, though in close proximity to the target, remained anatomically intact and did not show treatment-related changes (Fig. 2f). There were no tracks of megavoltage mini beam present in the region of the brain traversed by the beam (the dose given through each beamlet was approximately 50% of the prescription dose to the target, i.e., 13 Gy). Specific immunostaining showed infiltration by T lymphocytes and plasma cells in the MBRT group while this was nearly absent in the control group (Fig. 3).

DISCUSSION

In this study, all dogs treated with MBRT showed a response. Among this group 71% achieved complete pCR, with no residual tumor on postmortem study, in comparison to control group (standard radiation treatment) where dogs showed only partial response at best. The persistence of tumors after the treatment noted in the standard radiation treatment group, was similar to the tumor responses observed in the studies done in the past (6–8). The long-term treatment related changes seen in the standard radiation treatment group such as extensive vacuolization in brain parenchyma, encephalomalacia and rarefaction of vessels were similar to the findings reported in the literature (6–9).

In the MBRT group, the late-radiation-induced changes were mostly confined to areas that received >50% of the dose. There was no cellular or anatomical architectural damage related to treatment noted in the path of the MBRT beam. The findings from XFI provide insight into the distribution and concentration of elements, providing a measure of the metabolic state (including ion concentrations) in the tissue and demonstrate if there is any detectable damage to healthy brain. XFI results confirm that there is no detectable damage to healthy brain even in both entry and exiting paths of the mini beams. On neuropathological evaluation, the lethal treatment effects were seen only in the areas where spatially fractionated arrays of beams were intersected to overlap each other, which was planned with the intention of achieving more treatment effect in the target region. Despite the tissue destruction in the form of pan-necrosis (necrosis of cells and neuropil), it was confined mostly to the targeted area, and there were findings suggestive of cellular regeneration and recovery close to the area outside the targeted region. Neuropil recovery was noted within millimeters from the ablated target. By contrast in the control dogs, the late radiation changes in the brain, including microvacuolation and encephalomalacia, were noted in the areas that received doses <50% of the target area dose.

Downloaded From: https://bioone.org/journals/Radiation-Research on 11 Aug 2024
Terms of Use: https://bioone.org/terms-of-use

Radiation produces both neuropil injury and vascular injury. Encephalomalacia, or necrotic brain, can be seen with many causal origins which can be due to either vascular etiology and/or direct neuropil effect of high-energy photons. Evidence of both can be found in standard radiation treatment dogs in this study. In addition, tumor response to the radiation might be adduced from the lymphocyte infiltration. Supporting this idea was our finding of differential lymphocytes infiltration seen between MBRT and standard radiation treatment groups. The macrophage infiltration by contrast was more causally related to the necrosis.

Lymphocyte infiltration confined to the area of treatment after a single large dose open beam treatment has been reported (10) and presumed to be part of neuroinflammation response. The long standing neuroinflammation noted in this study shows that there is a possibility of long-term memory for immune system surveillance against tumor recurrence. Eloquent studies by Bouchet et al., showed the possibility that the tumoricidal effect of spatially fractionated doses may be mediated through immune modulation involving a complex network of mediators (32, 33). Interestingly, our study has shown more diffuse lymphocyte infiltration in the targeted region for MBRT patients, both perivascularly as well in the parenchyma outside the targeted area, which was not seen in the control group. This raises the possibility of immune modulation as a possible mechanism for the impressive results noticed with MBRT, however these results cannot conclusively determine the mechanism(s) responsible for pCR in MBRT patients. Immune modulation also possibly explains the exceedingly early response noted in the dog that was euthanized within 48 hours after treatment in the MBRT group. There are currently multiple hypothesis regarding the precise mechanism of action that leads to improved outcomes from synchrotron based micro or mini-beam treatments, none of which have been able to fully explain the outcomes (13, 14, 21–23). Similarly regarding MBRT generated on a linear accelerator, the immune modulation may play a role as one of the main mechanistic effects of MBRT that results in improved tumor cell destruction and related long-term effects noticed on normal brain tissue. However, a full explanation of the immune effects occurring during MBRT is beyond the scope of this work.

Results similar to those reported here have been shown for SMBRT where a study comparing SMBRT to synchrotron-generated open beam treatment for brain tumor has shown better tumor response with micro-beams (34). Despite this, MBRT clearly shows superior tumoricidal effects compared to standard radiation treatment with a significant sparing of damage to normal tissue.

Beam width of micro-beams may have significant impact on the tissue-sparing ability. A study comparing spatially fractionated beams with widths ranging between 200–800 μm, showed more uniform cellular necrosis including mature vasculature compared to beams with width <100 μm, where cellular necrosis involved specifically immature vasculature in zebrafish (35). However, another study (36) showed vascular normalization irrespective of beam width or dose, presumably from pericyte activation. In our study the beam width was kept to 1,000 μm in size, and no cellular damage noted in the beam path (both entrance and exit path). Our study finding is also contrary to a study using deuteron micro-beams, which showed destruction of normal tissue with 1,000 μm beams (37). The differences between synchrotron beam and megavoltage beam shape also results in a different dose to the interface between heavily irradiated peaks and nominally unirradiated valley tissues. Regenerative and reparative mechanisms possibly persist at this interface, as observed on microscopic examination as well as XFI, showing the regeneration of glial fabric and neural cell preservation very close to the targeted region just outside the intersected mini beams (Fig. 2c and f). Therefore, it can be speculated that the efficacy of these mechanisms may be different for megavoltage beams compared to synchrotron beams. Tissues irradiated with megavoltage mini beams will have a larger peak-to-valley interface region that receives a partial dose compared to tissues irradiated with SMBRT which has a sharper interface between peak and valley. This work shows delivering radiation in a spatially fractionated array of beamlets in a fashion similar to SMBRT, unlike the uniform dose delivery with standard conventional radiation treatment, would achieve superior tumor cell kill while preserving normal anatomy resulting in less tissue damage or side effects.

Studies have alluded (38, 39) to the feasibility of 2 interlacing micro-beams to deliver a large ablative dose to the target while exploiting the use of the tissue-tolerating effect of micro-beams in their path, before and after the intersection. One such study (39) hypothesized that the interlacing of the beams might allow for dose reduction, while achieving the same biological effect on the tumors. The positive effects of intersecting mini beams were achieved in this study where pan-necrosis was noticed in the area where 2 MBRT beams were intersected in the tumor-bearing targeted region. Just 26 Gy mean dose was applied in a single fraction to completely ablate the tumor (pCR 71%).

Use of more than one intersecting, non-parallel opposed MBRT beams would help encompass the target with a near-total prescribed dose, with relatively lower entry and exit doses. The main goal of this approach is to ablate the tumor in its entirety, while attempting to preserve normal structures. Two or more non-parallel MBRT beams, used to intersect over the target region appear to achieve this aim, as the entrance and exit beam paths will still have the peak-to-valley dose ratio maintained (from 50% to 30% i.e., from 0 cm to 10 cm depth) (25). The postmortem analysis of the brains of MBRT dogs show minimal to no radiation-induced damage in both the beam entrance and exit path, unlike the control dogs treated with a more uniform dose.

Downloaded From: https://bioone.org/journals/Radiation-Research on 11 Aug 2024
Terms of Use: https://bioone.org/terms-of-use

This new therapeutic modality does have few caveats including, limited use of gantry angles (degrees of freedom), the collimator itself needs to be manually attached to linear accelerator head, and requires a large number of monitor units to deliver the desired dose as the collimator output factor is low. However, these issues may not translate to major disadvantage for MBRT pending further development of the technology.

CONCLUSION

This is the first randomized study using MBRT generated on a linear accelerator with 1,000 μm size beams to treat *de novo* brain tumors in larger animals with a gyrencephalic brain. Findings in larger gyrencephalic brains with *de novo* tumors may be more closely applicable to the human brain, compared to findings from the lissencephalic brains of rodent animals such as rats or mice with transplanted tumors in their brain. The findings in this study reflect the long-term treatment outcome including both tumor control and late treatment-related effects on brain. The findings of MBRT have been discussed considering the published SMBRT work found in the literature.

This study using pet dogs which unlike human patients, are not cared for medically from the point of disease progression to death. Instead, they were euthanized at the discretion of their owners depending on social and emotional factors. This makes the survival or progression-free interval assessment impossible to discern. Nevertheless, this study showed an impressive 71% pCR in the study arm with 0% pCR in control arm, indicating clear therapeutic superiority of MBRT. In addition, the study also showed sparing of normal tissue in the study arm, compared to the control arm, highlighting the superior therapeutic ratio. The superior therapeutic results noted with MBRT including both tumor control, and normal structural preservation in the presence of neuroinflammation suggests the possibility of an immune-related mechanism in both therapy and toxicity. This justifies a potential scope for using immune modulatory agents, along with MBRT in the treatment of brain tumors. MBRT produced on a linear accelerator offers greater equipment accessibility to explore further treatment/clinical trial opportunities.

ACKNOWLEDGMENTS

We thank Dr Barbara E Powers, DVM, PhD, DACVP. (Veterinary Pathologist) for her invaluable support and time reporting on all the brain specimens of the dogs treated on this study. We thank Dr. Viktor Zherebitskiy, MD, FRCPC, ABP9NP/AP), FACP, FASCP (Neuropathologist) for his invaluable administrative support for this work. Synchrotron-based X-ray fluorescence imaging (XFI) was performed at the Stanford Synchrotron Radiation Lightsource (SSRL). The Stanford Synchrotron Radiation Lightsource, SLAC National Accelerator Laboratory, is supported by the U.S. Department of Energy, Office of Science, Office of Basic Energy Sciences under Contract No. DE-AC02-76SF00515. The SSRL Structural Molecular Biology Program is supported by the DOE Office of Biological and Environmental Research, and by the National Institutes of Health, National Institute of General Medical Sciences (P30GM133894). This work was supported by a grant from Saskatchewan Cancer Agency (OGF 414311). Neuropathology evaluation was supported by Mrs. J. Olszewska Neuropathology Fund.

Received: May 13, 2021; accepted: April 22, 2022; published online: May 10, 2022

REFERENCES

1. Perry JR, Laperriere N, O'Callaghan CJ, Brandes AA, Menten J, Phillips, et al. Short-Course Radiation plus Temozolomide in Elderly Patients with Glioblastoma. N Engl J Med. 2017; 376:1027-37.
2. Stupp R, Mason WP, van den Bent MJ, Weller M, Fisher B, Taphoorn MJ, et al. Radiotherapy plus concomitant and adjuvant temozolomide for glioblastoma. N Engl J Med. 2005; 352:987-96
3. Stupp R, Hegi ME, Mason WP, van den Bent MJ, Taphoorn MJ, Janzer RC, et al. Effects of radiotherapy with concomitant and adjuvant temozolomide versus radiotherapy alone on survival in glioblastoma in a randomised phase III study: 5-year analysis of the EORTC-NCIC trial. Lancet Oncol. 2009; 10:459-66.
4. Greene-Schloesser D, Robbins ME, Peiffer AM, Shaw EG, Wheeler KT, Chan MD, et al. Radiation-induced brain injury: A review. Front Oncol. 2012; 2:73.
5. Nagtegaal SHJ, David S, Snijders TJ, Philippens ME, Leemans A, Verhoeff JJ. Effect of radiation therapy on cerebral cortical thickness in glioma patients: Treatment-induced thinning of the healthy cortex. Neuro-oncol adv. 2020; 2:1-8.
6. Kelsey KL, Gieger TL, Nolan MW. Single fraction stereotactic radiation therapy (stereotactic radiosurgery) is a feasible method for treating intracranial meningiomas in dogs. Vet Radiol Ultrasound. 2018; 59:632-8.
7. Mariani CL, Schubert TA, House RA, Wong MA, Hopkins AL, Barnes Heller HL, et al. Frameless stereotactic radiosurgery for the treatment of primary intracranial tumours in dogs. Vet Comp Oncol. 2015; 13:409-23
8. Griffin LR, Nolan MW, Selmic LE, Randall E, Custis J, LaRue S. Stereotactic radiation therapy for treatment of canine intracranial meningiomas. Vet Comp Oncol. 2016; 14: e158-e170.
9. David S, Mesri HY, Bodiut VA, Nagtegaal SH, Elhalawani H, de Luca A, et al. Dose-dependent degeneration of non-cancerous brain tissue in post-radiotherapy patients: A diffusion tensor imaging study. medRxiv. 2019; 19005157:1-24.
10. Moravan MJ, Olschowka JA, Williams JP, O'Banion MK. Cranial irradiation leads to acute and persistent neuroinflammation with delayed increases in T-cell infiltration and CD11c expression in C57BL/6 mouse brain. Radiat Res. 2011; 176:459-73.
11. Goncharov NV, Nadeev AD, Jenkins RO, Avdonin PV. Markers and biomarkers of endothelium: when something is rotten in the state. Oxid Med Cell Longev. 2017; 2017:1-27.
12. Anschel DJ, Romanelli P, Benveniste H, Foerster B, Kalef-Ezra J, Zhong Z, et al. Evolution of a focal brain lesion produced by interlaced microplanar X-rays. Minim Invasive Neurosurg. 2007; 50:43-6.
13. Slatkin DN, Spanne P, Dilmanian FA, Gebbers JO, Laissue JA. Subacute neuropathological effects of microplanar beams of x-rays from a synchrotron wiggler. Proc Natl Acad Sci USA. 1995; 92:8783-7.
14. Dilmanian FA, Button TM, Le Duc G, Zhong N, Peña LA, Smith JA, et al. Response of rat intracranial 9L gliosarcoma to microbeam radiation therapy. Neuro Oncol. 2002; 4:26-38.
15. Serduc R, Bouchet A, Bräuer-Krisch E, Laissue JA, Spiga J, Sarun S, et al. Synchrotron microbeam radiation therapy for rat brain tumor palliation-influence of the microbeam width at constant valley dose. Phys Med Biol. 2009; 54:6711-24
16. Coderre J, Rubin P, Freedman A, Hansen J, Wooding Jr TS, Joel

Downloaded From: https://bioone.org/journals/Radiation-Research on 11 Aug 2024
Terms of Use: https://bioone.org/terms-of-use

D, et al. Selective ablation of rat brain tumors by boron neutron capture therapy. Int J Radiat Oncol Biol Phys. 1994; 28:1067-77.

17. Bräuer-Krisch E, Serduc R, Siegbahn EA, Le Duc G, Prezado Y, Bravin A, et al. Effects of pulsed, spatially fractionated, microscopic synchrotron X-ray beams on normal and tumoral brain tissue. Mutat Res. 2010; 704:160-6.
18. Anschel DJ, Bravin A, Romanelli P. Microbeam radiosurgery using synchrotron-generated submillimetric beams: a new tool for the treatment of brain disorders. Neurosurg Rev. 2010; 34:133-142.
19. Serduc R, Vérant P, Vial JC, Farion R, Rocas L, Rémy C, et al. In vivo two-photon microscopy study of short-term effects of microbeam irradiation on normal mouse brain microvasculature. Int J Radiat Oncol Biol Phys. 2006; 64:1519-27.
20. Ricard C, Fernández M, Gastaldo J, Dupin L, Somveille L, Farion R, et al. Short-term effects of synchrotron irradiation on vasculature and tissue in healthy mouse brain. J Synchrotron Radiat. 2009; 16:477-83.
21. Bouchet A, Lemasson B, Le Duc G, Maisin C, Bräuer-Krisch E, Siegbahn EA, et al. Preferential effect of synchrotron microbeam radiation therapy on intracerebral 9L gliosarcoma vascular networks. Int J Radiat Oncol Biol Phys. 2010; 78:1503-12.
22. Bouchet A, Serduc R, Laissue JA, Djonov V. Effects of microbeam radiation therapy on normal and tumoral blood vessels. Phys Med. 2015; 31:634-41.
23. Dal Bello R, Becher T, Fuss MC, Krämer M, Seco J. Proposal of a chemical mechanism for mini-beam and micro-beam efficacy. Front Phys. 2020; 8:564836.
24. Babcock K, Sidhu N, Kundapur V, Ali K. Collimator design for experimental minibeam radiation therapy. Med Phys. 2011; 38:2192-7.
25. Cranmer-Sargison G, Crewson C, Davis WM, Sidhu NP, Kundapur V. Medical linear accelerator mounted mini-beam collimator: design, fabrication and dosimetric characterization. Phys Med Biol. 2015; 60:6991-7005.
26. Alexander A, Crewson C, Davis W, Mayer M, Cranmer-Sargison G, Kundapur V. Treatment planning study for spatially fractionated minibeam radiotherapy. Radiother Oncol. 2016; 119:S414.
27. Davis W, Crewson C, Alexander A, Kundapur V, Cranmer-Sargison G. Dosimetric characterization of an accessory mounted mini-beam collimator across clinically beam matched medical linear accelerators. Biomed. Phys. Eng. Express. 2017; 3:015015.
28. Schiffman JD, Breen M. Comparative oncology: what dogs and other species can teach us about humans with cancer. Philos Trans R Soc Lond B Biol Sci. 2015; 370:1673.
29. Pushie MJ, Sylvain NJ, Hou H, Caine S, Hackett MJ, Kelly ME. Tracking elemental changes in an ischemic stroke model with X-ray fluorescence imaging. Sci Rep. 2020; 10: 17868.
30. MicroAnalysis Toolkit, SMAK. https://www.sams-xrays.com/smak
31. Tiller-Borcich J, Fike J, Phillips T, Davis R. Pathology of delayed radiation brain damage: an experimental canine model. Radiat Res. 1987; 110:161–172.
32. Bouchet A, Sakakini N, El Atifi M, Le Clec'h C, Brauer E, Moisan A, et al. Early gene expression analysis in 9L orthotopic tumor-bearing rats identifies immune modulation in molecular response to synchrotron microbeam radiation therapy. PLoS One. 2013; 8: e81874.
33. Bouchet A, Sakakini N, El Atifi M, Le Clec'h C, Bräuer-Krisch E, Rogalev L, et al. Identification of AREG and PLK1 pathway modulation as a potential key of the response of intracranial 9L tumor to microbeam radiation therapy. Int J Cancer. 2015; 136:2705-16.
34. Bouchet A, Bräuer-Krisch E, Prezado Y, El Atifi M, Rogalev L, Le Clec'h C, et al. Better efficacy of synchrotron spatially microfractionated radiation therapy than uniform radiation therapy on glioma. Int J Radiat Oncol Biol Phys. 2016; 95:1485-94.
35. Brönnimann D, Bouchet A, Schneider C, Potez M, Serduc R, Bräuer-Krisch E, et al. Synchrotron microbeam irradiation induces neutrophil infiltration, thrombocyte attachment and selective vascular damage in vivo. Sci Rep. 2016; 6:33601.
36. Griffin RJ, Koonce NA, Dings RP, Siegel E, Moros EG, Bräuer-Krisch E. Microbeam radiation therapy alters vascular architecture and tumor oxygenation and is enhanced by a galectin-1 targeted anti-angiogenic peptide. Radiat Res. 2012; 177:804-812.
37. Curtis HJ. The biological effects of heavy cosmic ray particles. Life Sci Space Res. 1963; 1:39-47.
38. Bräuer-Krisch E, Requardt H, Régnard P, Corde S, Siegbahn E, Le Duc G, et al. New irradiation geometry for microbeam radiation therapy. Phys Med Biol. 2005; 50:3103-11.
39. Dilmanian FA, Zhong Z, Bacarian T, Benveniste H, Romanelli P, Wang R, et al. Interlaced x-ray microplanar beams: a radiosurgery approach with clinical potential. Proc Natl Acad Sci USA. 2006; 103:9709-14.

Downloaded From: https://bioone.org/journals/Radiation-Research on 11 Aug 2024
Terms of Use: https://bioone.org/terms-of-use